DALTON
PERSPECTIVE

Insights from protein film voltammetry into mechanisms of complex biological electron-transfer reactions †

Fraser A. Armstrong

Inorganic Chemistry Laboratory, Department of Chemistry, Oxford University, South Parks Road, Oxford, UK OX1 3QR

Received 14th September 2001, Accepted 16th October 2001
First published as an Advance Article on the web 24th January 2002

As the fundamental principles of long-range electron transfer (ET) in proteins are becoming well understood, interest is focusing on the mechanisms by which ET is coupled to chemical reactions such as ion transport and catalysis. Protein film voltammetry provides a powerful way to investigate these problems. The protein is immobilised on an electrode as an adsorbed electroactive film, typically a monolayer or less: then, by applying a potential, electrons are driven in and out of the active sites, resulting in diagnostically useful current signals. It is possible to resolve complex reactions over a wide dynamic range. For example, with cyclic voltammetry, scan rates exceeding 1000 V s^{-1} can be used to observe coupling reactions that occur in the sub-millisecond time domain. For enzymes, catalysis can be measured as a function of potential to reveal processes that are mechanistically informative and may be involved in controlling activity. This paper will illustrate the capabilities of this approach for mechanistic investigations into biological redox chemistry.

Introduction

In enzymes and many other proteins, the redox properties of transition metals have been exploited to perform some of the most sophisticated chemistry known. Long-range electron-transfer (ET) has long been an important topic for biological sciences, particularly bioenergetics; but as the fundamental principles become better understood, interest is focusing increasingly on the ways in which ET is *coupled—i.e.* linked to *chemical* reactions. In redox catalysis, energy transduction and many aspects of regulation, ET drives ligand (substrate) binding, ion (proton) transfer, and protein conformational changes, while in turn ET can also be gated by these processes. However, the mechanisms by which these reactions interrelate to produce an optimised and harmonised system are difficult to determine.

† Based on the presentation given at Dalton Discussion No. 4, 10–13th January 2002, Kloster Banz, Germany.

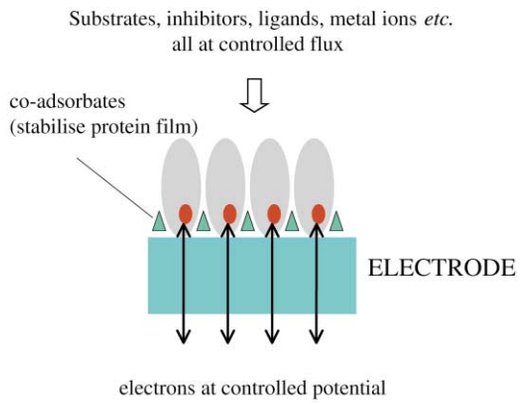

Fig. 1 Cartoon showing an adsorbed monolayer of protein molecules on an electrode.

Protein film voltammetry provides a powerful way to investigate the mechanisms of ET coupling.[1] As indicated in Fig. 1, the sample is configured on a suitable electrode surface as a stable mono-/submono-layer film of protein molecules, each capable of facile electron transfer. Although these molecules will retain some mobility (perhaps 'rocking' motions that change their orientations) the problems of sluggish diffusion and kinetics of encounter at the electrode are essentially overcome: it therefore becomes possible to exploit the unique abilities of dynamic electrochemical methods to control, detect and quantify the complex, redox-coupled chemical reactions that occur at the active sites. Experiments may be carried out over a wide range of timescales to view both transient and steady-state processes occurring in the same sample. This paper will give a brief overview of recent applications of protein film voltammetry in the elucidation of some complex mechanistic problems in biological redox chemistry. We will focus particularly on a few examples that either show how data are analysed, or illustrate the detection of interesting phenomena that are as yet unresolved.

Fraser Armstrong

Fraser Armstrong gained his PhD in 1978 at the University of Leeds, under the supervision of A. Geoffrey Sykes. He then held a Royal Society European Exchange Fellowship with Peter Kroneck at the University of Konstanz, Germany. After further postdoctoral research with Ralph Wilkins (New Mexico State University), Helmut Beinert (Institute for Enzyme Research, Madison, Wisconsin) and Allen Hill (Oxford), he took up a Royal Society University Research Fellowship at Oxford in 1983. In 1989 he joined the faculty at the Department of Chemistry, University of California, Irvine. He returned to Oxford in 1993, where he is now Professor of Chemistry and a Fellow of St. John's College. His interests are in biological redox chemistry, in particular the application of dynamic electrochemical methods to determine mechanisms of complex electron transfer and catalytic reactions in proteins. He has recently been awarded the 1998 European Medal for Biological Inorganic Chemistry and the 2000 Royal Society of Chemistry award for Inorganic Biochemistry.

To be effective, the native structural and reactivity characteristics of the protein must be retained in the adsorbed state; so it is necessary that the redox centres should act homogeneously and independently of each other, and remain fully accessible to ions and small reagents in the contacting electrolyte. The large size of protein molecules suggests these requirements should be easily satisfied; *i.e.* active sites are likely to be well separated from those in neighbouring molecules, and the layer should be porous to small ions and molecules. Importantly, by contrast with the attachment of small molecules to an electrode, there is a much better chance that an active site that is shielded by surrounding polypeptide will retain the properties it has in free solution, and indeed there are now many examples for which it is certain that no significant changes occur upon adsorption. Retention of a characteristic activity like catalysis is a useful criterion; but adsorbed proteins can often be examined independently by spectroscopic methods; in particular, surface-enhanced Raman and resonance Raman, UV and visible reflectance, and UV-visible absorption using metallic or optically transparent electrodes.[2–4] These techniques have been used mostly for haemoproteins, which show intense and well-defined vibrational and electronic bands.

i) The redox status of the entire sample can be fine-tuned. All the redox centres in the sample are controlled directly by the electrode potential, and a much higher degree of control over reactivities is obtained compared to conventional experiments which address freely diffusing molecules.

ii) Waveform definition. In linear sweep or cyclic voltammetry, a layer of molecules undergoing simple reversible ET gives a signal consisting of a pair of compact reduction and oxidation peaks (Fig. 2A) each having a half-height width

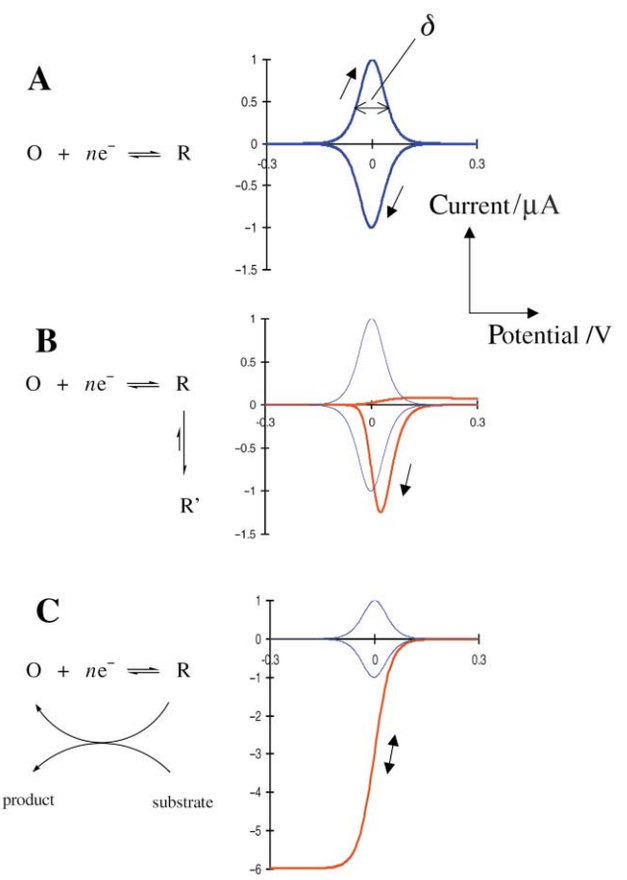

Fig. 2 Voltammograms expected for adsorbed redox couples displaying different types of ET coupling. **A**. Reversible ET. **B**. Red trace shows ET coupled to a spontaneous chemical reaction of the reduced form; on this timescale, the reverse chemical process gates electron transfer. Blue trace shows uncoupled ET for comparison. **C**. Red trace shows ET coupled to catalytic regeneration of oxidised form. Blue trace shows uncoupled ET.

$\delta = 83/n$ mV at 0 °C (δ is usually larger than this due to inhomogeneity) the areas of which relate easily to the number of centres undergoing reaction.[5] The average value of the oxidation and reduction peaks gives the reduction potential, while their changes in shape and separation as the scan rate is increased yields information on the ET kinetics—most directly, the standard electron-transfer rate constant k_0 (the exchange rate at the formal reduction potential).

iii) Efficient screening for reactivities. The protein-coated electrode can be transferred between different solutions, effecting an 'instantaneous pico-dialysis' that rapidly subjects the redox centres to different environments, even extremes of pH or alternative solvents, in which the protein would normally denature in a more prolonged operation.

iv) Sample economy. Theoretically, the amount of sample required is only that needed to form up to a monolayer, typically in the range 10^{-12} to 10^{-11} mol cm^{-2}.

v) Sensitivity and stoichiometry. The minuscule sample size (but note the local concentration is very high) allows the investigation of coupled reactions that occur with very low (trace) levels of agents in the contacting electrolyte.

vi) Fast reactions. Since the voltammetric waveform and current are not limited by diffusion or encounter with the electrode, the specific chemical reactions of the protein's active site(s) come into better focus. Roughly speaking, a standard ET rate constant of 500 s^{-1} or higher enables us to address redox-coupled chemical reactions with half-lives less than a millisecond.

Coupling of electron transfer to a chemical process (known in electrochemistry as an 'EC' reaction) is usually described by a simple square scheme.[6] The voltammetric waveshape can vary depending on the values of different parameters: for example, the situation shown in Fig. 2B is that of an electron transfer followed by a spontaneous chemical process that results in a product for which re-oxidation depends upon a relatively slow reverse chemical process. This behaviour will be illustrated later in the context of proton coupling and ligand exchange at metal centres.

As shown in Fig. 2C, catalytic turnover may cause the peak-like signal to convert to a sigmoidal wave with a limiting (plateau) current that is independent of potential. More generally, the waveforms that arise from a catalytic reaction depend on many factors. With a normal flat macro-electrode having a high coverage of very active enzyme, the limiting current may be controlled by the transport of substrate and will show a square-root dependence on electrode rotation rate.[7] As the coverage or activity decreases, or if the electrode is a microelectrode or one that is rotating at high frequency, the waveform will more likely be determined by electron transfer or catalytic properties of the enzyme, and the limiting current will relate directly to turnover rate. The data derived by varying electrode rotation rate, coverage and substrate concentration should produce the expected kinetic constants (turnover number and Michaelis constant) for the enzyme, thereby indicating that the enzyme's properties have not been altered in the adsorbed state. Other more intricate properties of the enzyme can then be probed; for example, catalytic activity may depend in an unusual way on potential, due to key stages being facilitated for particular oxidation states.

In our own work, we have made particular use of the pyrolytic graphite 'edge-plane' (PGE) electrode. This has proven useful for a wide variety of proteins, most likely because it is easily polished; using abrasives such as alumina to produce a rough hydrophilic surface rich in acidic C–O functionalities.[8] Among other important electrodes, we can distinguish those in which Au (or Ag) is modified with a self-assembled monolayer (SAM) of alkanethiols or terminally functionalised alkanethiols.[9] These offer superb capabilities for controlling surface chemistry, and ET distance, and are suitable for informative spectroscopic studies.

Electron transfer characteristics of adsorbed proteins

Before turning to examples that illustrate the mechanistic insight that can be obtained into specific types of active-site ET coupling, we shall first consider whether even 'simple' systems show straightforward behaviour. The Butler–Volmer model for electrochemical kinetics predicts that increasing the driving force (over-potential) should raise the rate of electron transfer exponentially, while the Marcus theory states, more precisely, that this relationship should hold up to potentials approaching that of the reorganization energy of the system. Therefore it is interesting to note that studies carried out so far with different proteins adsorbed on various electrodes have suggested that ET is 'capped' at values far below those expected.

Niki and co-workers have found that the rate of electron transfer for cytochrome c adsorbed at Au electrodes modified with a carboxy-terminated alkylthiol SAM appears to reach a limiting plateau as the chain length is decreased, and they have suggested that ET may depend upon the rate of attainment of optimal orientations on the electrode.[10] This is similar to ideas put forward for the 'gating' of inter-protein ET reactions, in which the rate is controlled by attainment of a specific bimolecular configuration.[11] Murgida and Hildebrandt have also observed 'gating' for cytochrome c adsorbed on a SAM-modified Ag electrode, using FTIR detection of the active-site redox-linked vibrational bands: here, however, there is a marked H/D solvent isotope effect, prompting the authors to propose a mechanism involving rearrangement of internal H-bonds as the electron is transferred.[12] Likewise for Azurin, a 'blue' Cu protein, there is evidence that ET rates at different electrodes are limited by a process with a rate constant $<10^4$ s^{-1}.[13] Whatever, their origin, these reactions may place an upper rate limit on the specific active-site coupled kinetics that we wish to study. For comparison, studies on ferrocene covalently attached to π-conjugated thiol SAMs have shown that extremely high ET rates can be obtained even for long-chain lengths.[14]

Gated electron transfer at protein active sites

A specific example of ET coupling in proteins is redox-linked proton transfer, *i.e.* where a change in oxidation state of a redox centre is linked to transfer of a proton. A mechanistic problem arises if the proton-binding site is buried and isolated from solvent water molecules, since whereas an electron can easily tunnel more than 10 Å, a proton at the same energy is limited to hops of less than 0.25 Å.[15] Consequently, long-range proton transport within a protein requires a chain of closely-spaced mediators—donors and acceptors (water molecules or amino acid side chains) whose separation and p*K* values control the flow rate. The connections in this 'proton relay' may depend on protein motions that 'swing' one group towards another;[16] however, the large membrane-bound proton-pumping enzymes are not defined at sufficiently high resolution or in all the relevant states to obtain a precise structural description of the mechanism.[17]

By contrast, some detailed insight is provided by recent studies we have carried out on a small Fe-S protein, ferredoxin I (FdI) isolated from the nitrogen fixing bacterium *Azotobacter vinelandii* (*A.v.*).[18–20] Ferredoxin I (MW 12 kDa) contains two clusters, one [4Fe-4S] and one [3Fe-4S], the latter undergoing a one-electron transfer that is coupled to proton transfer as shown in Scheme 1. This system provides a good example of how protein film voltammetry is applied to unravel a complex mechanism.

As shown in Fig. 3, the $[3Fe\text{-}4S]^{+/0}$ cluster has a pH-dependent reduction potential, consistent with the binding of a single proton in the reduced ('0') state.[18,21] This is supported by results from spectroscopy, crystallography and site-directed mutagenesis, and it is likely that protonation occurs on one of the μ-sulfido groups.[21–24]

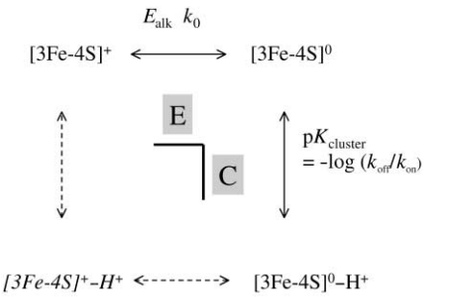

Scheme 1 Square scheme depicting electron and proton binding to the [3Fe-4S] cluster of *Azotobacter vinelandii* ferredoxin I. There is no evidence for participation of the species $[3Fe\text{-}4S]^{1+}$–H^+, thus only two sides of the square are used. The electrochemical reaction is of the familiar 'EC' type.

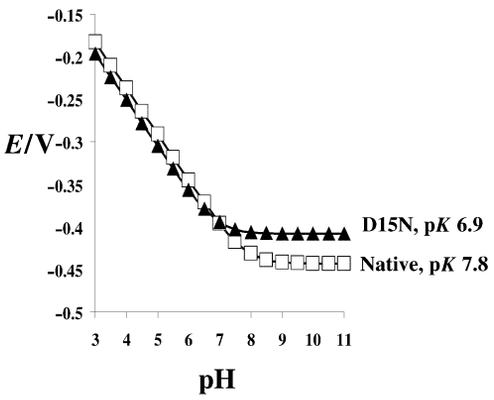

Fig. 3 The pH dependences of the $[3Fe\text{-}4S]^{+/0}$ reduction potential in *Azotobacter vinelandii* ferredoxin I, showing lines constructed for native and D15N mutant forms based upon the parameters shown in respective boxes (see also Scheme 1).

High-resolution structures (1.4 Å) have been obtained for both oxidised ($[3Fe\text{-}4S]^+$) and reduced ($[3Fe\text{-}4S]^0$) forms of *A.v.* FdI at high and low pH.[25–27] Fig. 4 shows the region around the [3Fe-4S] cluster which is buried some 7–8 Å below the protein surface: the intervening space contains no water molecules to act as proton mediators yet proton exchange with solvent is fast. This raises the question of how the proton can move so efficiently into the protein in response to a change in oxidation state—a problem central to bioenergetics and proton-pumping enzymes. An important clue to this problem is that the carboxylate side-chain of aspartate-15 (D15), which is surface-exposed and salt-bridged with the side chain $–NH_4^+$ from lysine (K)-84, lies some 5 Å from the cluster, and rotates about 90° when the cluster is reduced at pH values above 8.[26]

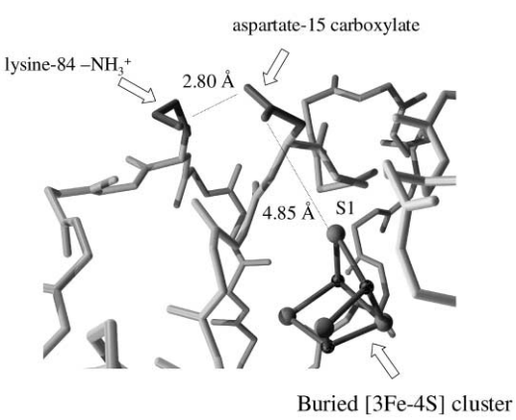

Fig. 4 Structure in the vicinity of the buried [3Fe-4S] cluster in *Azotobacter vinelandii* ferredoxin I, showing the positions of aspartate-15 that facilitates proton transfer to and from the solvent, and of the closest sulfur atoms of the cluster (S1). Based upon data given in refs. 25–27.

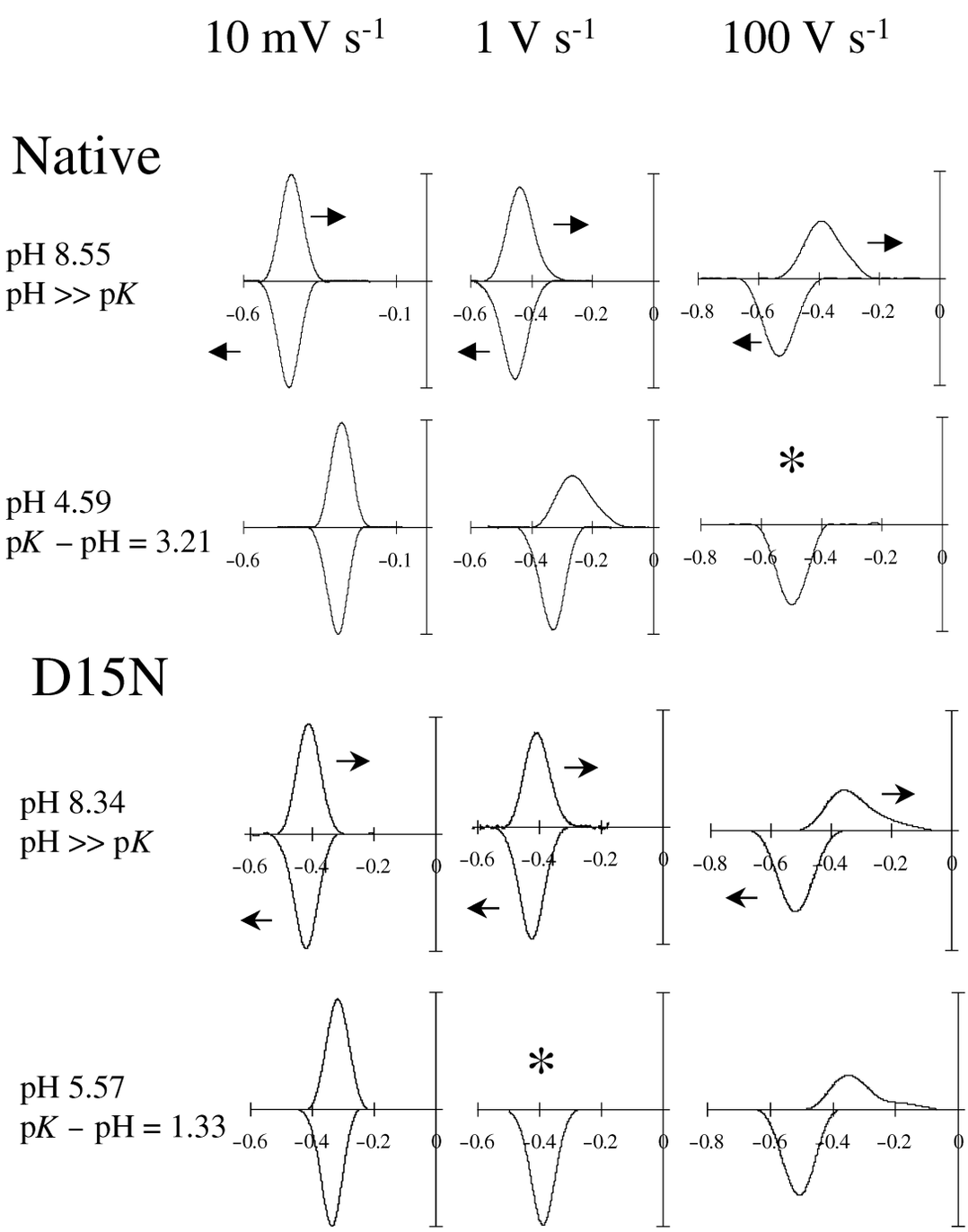

Fig. 5 Voltammograms of the $[3Fe\text{-}4S]^{+/0}$ couple in native and D15N mutant forms of *Azotobacter vinelandii* ferredoxin adsorbed on a PGE electrode. In each case the cycle is commenced from the oxidised state. The results show how the oxidation reaction is 'gated' in different time domains (*) by proton transfer. Proton transfer is retarded in the D15N mutant, thus re-oxidation is not observed at 1 V s^{-1}, but reappears at 100 V s^{-1} because the proton does not reach the cluster during the cycle. For the native protein, proton transfer is much faster, and disappearance of the re-oxidation wave is observed instead at 100 V s^{-1}.

To elucidate the mechanism, several mutants of *A. v.* FdI were prepared: in some cases aspartate-15 was replaced by other amino acids; in others, residues apart from aspartate-15 that might be important were changed.[20] As evident from Fig. 3, replacement of aspartate-15 by asparagine lowers $pK_{cluster}$ for the $[3Fe\text{-}4S]^{0}$ form from 7.8 to 6.9, and the limiting $E^{o'}$ value (at high pH where no proton is transferred) increases from −430 mV to −409 mV.[18] This is as expected if a negative charge is removed a short distance from the cluster. In the low pH region the native and mutant forms have similar reduction potentials, reflecting the fact that the redox reaction is electroneutral ($e^- + H^+$) and thus little influenced by the presence of nearby charged residues.

Molecules of FdI adsorbed on PGE in the presence of polymyxin or neomycin (which stabilize the film) show fast interfacial electron exchange (k_0 is typically about 500 s^{-1}) and scan rates in the range 0.01–100 V s^{-1} resolve the coupled proton-transfer kinetics. The different variants fall into two categories: those displaying 'slow' or 'fast' proton-transfer kinetics.[20] Fig. 5 shows examples of the base-line subtracted cyclic voltammograms obtained for an example of either category, *i.e.* native (fast) and D15N (slow).[19] In each case the cycle is commenced after a brief polarisation period at the oxidising limit, *i.e.* referring to Scheme 1, the initial state is $[3Fe\text{-}4S]^{+}$ which cannot be protonated.

At high pH (pH > $pK_{cluster}$) no proton is transferred and the $[3Fe\text{-}4S]^{1+/0}$ signals of different variants are similar in appearance apart from some variation in $E^{o'}$, and they are reversible even at 100 V s^{-1}. (Note that some pH-independent asymmetry is evident at these high scan rates, although its origin is not

Table 1 Kinetic and thermodynamic parameters for the redox-driven proton transfer reaction at the [3Fe-4S] cluster of *Azotobacter vinelandii* ferredoxin I and different site-directed mutant variants. Adapted from ref. 20, with permission from the Nature Publishing Group

Variant	E_{alk}/V	p$K_{cluster}$ (high pH)	p$K_{cluster}$ (low pH)	k_{on}/M^{-1} s^{-1} [b] (pH 7.0)	k_{off}/s^{-1} [b] (pH 7.0)	pK_1	pK_2	k_{on}^{hop}/s^{-1}	k_{off}^{hop}/s^{-1}
FAST proton transfer									
Native	−0.443	7.8 ± 0.1	6.5 ± 0.1	7.9×10^9	308	7.2 ± 0.1	5.9 ± 0.1	1294 ± 100	332 ± 25
E18Q	−0.453	7.7 ± 0.1	6.7 ± 0.1	4.8×10^9	207	7.1 ± 0.1	6.1 ± 0.1	910 ± 90	230 ± 25
T14C	−0.464	8.4 ± 0.1	7.1 ± 0.1	6.6×10^9	207	8.0 ± 0.1	6.7 ± 0.1	720 ± 70	310 ± 25
K84Q	−0.476	8.1 ± 0.1	6.6 ± 0.1	9.0×10^9	232	7.4 ± 0.1	5.9 ± 0.1	1252 ± 100	250 ± 25
Native (D_2O)	−0.443	7.8 ± 0.1	6.5 ± 0.1	6.0×10^9	222	7.2 ± 0.1	5.9 ± 0.1	970 ± 100	240 ± 25
SLOW proton transfer		p$K_{cluster}$		k_{on}/M^{-1} s^{-1}	k_{off}/s^{-1}				
D15N	−0.408	6.9 ± 0.1		2.0×10^7	2.5 ± 0.1				
D15K-K84D	−0.397	6.6 ± 0.1		1.2×10^7	3.0 ± 0.1				
D15E	−0.388	6.7 ± 0.1		2.0×10^7	4.5 ± 0.2				

[a] All terms are as defined in Schemes 1 and 2. [b] For the fast reactions, $k_{on} = k_{on}^{hop}/([H^+] + K_1)$ and $k_{off} = k_{off}^{hop}\ K_2/([H^+] + K_2)$. Interaction with aspartate-15 causes the pK of the cluster to be different at high and low pH. In all cases k_0, the standard first-order electrochemical rate constant for electron exchange (at the reduction potential) is >200 s^{-1}, thus electron transfer is never rate-limiting.

known.) By contrast, at lower pH (pH < p$K_{cluster}$) where [3Fe-4S]^0 takes up a proton, the voltammetry depends critically on scan rate. At slow rates, the voltammograms appear reversible since all species (see Scheme 1) equilibrate with the electrode potential; thus $E^{o'}$ increases as the pH is lowered, as expected from Fig. 3. Then, as the scan rate is increased, the kinetics of the coupled proton transfer are revealed. We may refer back to Fig. 2B. Firstly, in certain time-domains, the re-oxidation process is gated (the oxidation peak vanishes as indicated by *). The 'slow' mutant D15N shows gating at 1 V s^{-1}, whereas with the native protein, gating is not observed until much higher rates (*e.g.* 100 V s^{-1}) are used. Secondly, for D15N and other slow mutants, the oxidation peak reappears as the scan rate is increased above 10 V s^{-1}, and we note that the voltammograms at 100 V s^{-1} are identical regardless of pH. Rapid sweeps to very positive potentials produced no evidence for any signal from the protonated redox couple H$^+$–[3Fe-4S]$^{1+/0}$. Therefore, referring to Scheme 1, the reaction involves only two sides of the square, *i.e.* oxidation of [3Fe-4S]^0–H$^+$ to [3Fe-4S]$^{1+}$ involves deprotonation followed by electron loss, and not the other way round.

The data are analysed by plotting peak positions (oxidation and reduction) against scan rate, and representative plots for native FdI and the D15N variant are shown in Fig. 6; in each case, the voltammograms were commenced from the oxidative limit. For a simple, uncoupled electron transfer, the peak potentials should separate symmetrically and give a trumpet-like shape.[28] Although we have termed these 'trumpet plots', it is the various deviations from this simple form that reveal the intricacies of the coupling reactions. The plot represents a *clock* in which the horizontal axis relates to the ET process in different time domains, in this case from several seconds down to milliseconds. Coupling distorts the plots in different regions and the resulting shapes can be modelled in terms of kinetic schemes of varying complexity. Here, in addition to the ET rate constant k_0, we needed to allow for the proton-transfer rate constants and pH-dependencies, participation of a base relaying the proton between solvent and cluster, and variations of the pK of both cluster and base during the reaction. At high pH the plots are simple, but they change dramatically as the pH is lowered. On the left hand side of each plot, *i.e.* in the long time-scale domain, the data resemble those of a potentiometric experiment, *i.e.* the system equilibrates with the electrode potential. By contrast, on the right hand side, the electrode potential can be cycled sufficiently fast (*e.g.* for D15N) that the reduction potential that is measured (the average of oxidation and reduction peaks) corresponds to a 'snapshot' of the system, trapped in the millisecond time domain. In an intermediate region, we observe the time-domain in which the oxidation is gated.

The data show that the electron and proton transfers must be *stepwise* events. Electron transfer *to* the cluster drives proton transfer, whereas electron transfer *off* the cluster is 'gated' by proton transfer. Electron transfer is rapid in all cases, so if the scan rate is fast enough, the [3Fe-4S] cluster can gain and release its electron before proton transfer can occur. The reduction potential apparently shifts in the negative direction as the scan rate is increased: this is because the proton does not have sufficient time to reach the cluster; so that the process being observed is the uncoupled [3Fe-4S]$^{1+/0}$ electron transfer, even under acidic conditions. The data for different pH values are expected to converge at high scan rates, and this is indeed observed for the 'slow' variants. Notably, for 'slow' mutants', a fast cycle (pH < p$K_{cluster}$) commenced from the reductive potential limit gives no voltammetric response because the cluster is trapped with a bound proton.

These results are supported by stopped-flow measurements, using $Fe(CN)_6^{3-}$ or $Ru(NH_3)_6^{3+}$ as oxidants.[19] In D15N, the rate of oxidation of the protonated [3Fe-4S]^0 cluster (at pH ≪ p$K_{cluster}$) is slow and pH independent; whereas with native FdI, oxidation is fast with a rate constant that decreases as the pH is lowered. In all cases the kinetics are independent of the oxidant, and replacement of H_2O by D_2O reveals only a small isotope effect, showing that proton tunneling is unlikely to be rate-determining.

Data for the different variants are given in Table 1, and we note first the absolute requirement for aspartate-15. The fast proton transfer observed for K84Q shows that the salt bridge between aspartate-15 and lysine-84 is unimportant. Notably, whereas the slow mutants conform to the simple kinetic model of Scheme 1, fitting the data for the fast mutants requires inclusion of an interaction between the cluster and the aspartate carboxylate so that after the electron has transferred to the cluster, the pK of the carboxylate *increases* (pK_1 ≫ pK_{OX}) to promote proton capture from solvent. The kinetic mechanism of proton transfer that emerges is shown in Scheme 2, which extends the simple thermodynamic cycle of Scheme 1. The ability of the carboxylate to sense and respond to the charge on the cluster is important in the electron–proton coupling mechanism. Once the proton has arrived at the cluster, the pK of the D15 carboxylate decreases from pK_1 to a value pK_2 that is similar to that observed when the cluster is oxidized (pK_1 ≫ pK_2 ≈ pK_{OX}): likewise, the cluster pK responds to the protonation state of the aspartate. In proton pumping enzymes, these

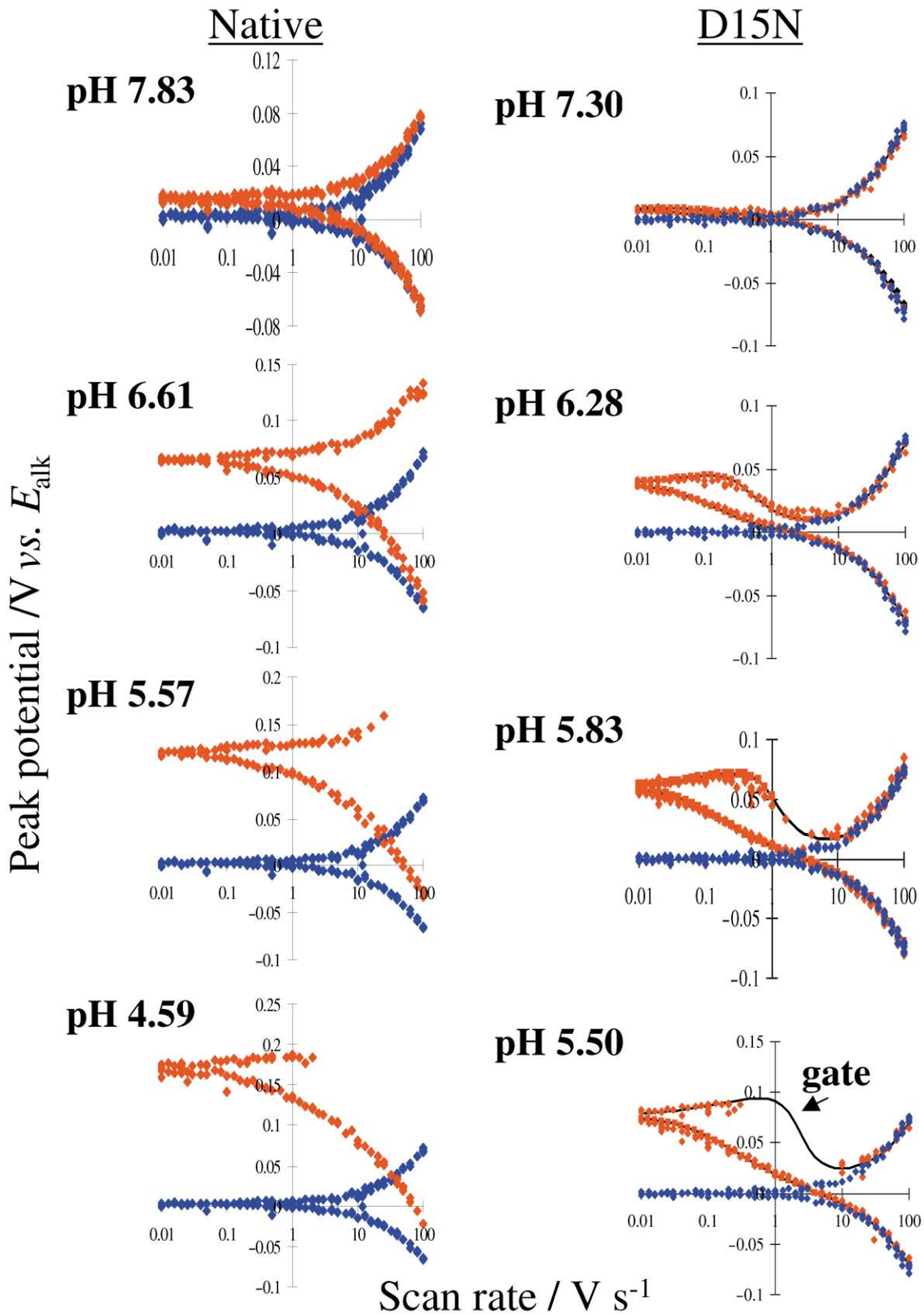

Fig. 6 Representative 'Trumpet Plots' for the [3Fe-4S]$^{+/0}$ couple in native and D15N mutant forms of *Azotobacter vinelandii* ferredoxin I adsorbed on a PGE electrode. The plots for D15N also show the fits based on k_{off} = 2.5 s^{-1}. Note the intermediate region of the plot (pH 5.50) in which an oxidation peak is not observed because ET is gated. Data points shown in red are for the pH values indicated whereas data points shown in blue are for the uncoupled electron-transfer reaction occurring at pH > p$K_{cluster}$.

redox-sensitive pK shifts may be very sizeable.[29] Table 1 includes values for the second-order rate constants for protonation, from which it is clear that the fast mutants approach the limit for diffusion control even though the cluster is buried. The similarity of rate constants for the slow mutants suggest a common mechanism—perhaps an improbable combination of breathing modes that allow temporary access for a H_2O molecule. Notably, introduction of another –CH_2– group into the aspartate-15 sidechain (D15E) renders it inactive in proton transfer.

Molecular dynamics computations show the resulting neutral –COOH group to be very mobile: it can penetrate the protein with high-frequency excursions (timescale 10^{-11} s), approaching to within hydrogen-bonding distance of the closest sulfur atom (S1) of the [3Fe-4S] cluster (see Fig. 4).[20] The carboxylate thus

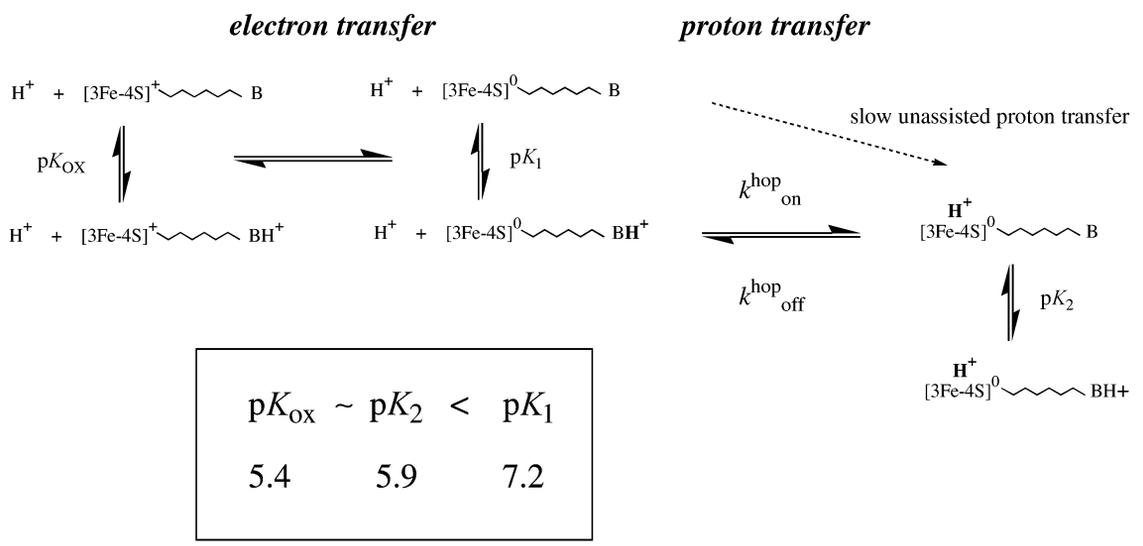

Scheme 2 Kinetic mechanism of proton transfer between bulk water and the [3Fe-4S] cluster in *Azotobacter vinelandii* ferredoxin I. Fast proton transfer to $[3Fe\text{-}4S]^0$ is pH dependent, and protonation constants of B (aspartate-15) are sensitive to whether the cluster is protonated or unprotonated. At low pH, aspartate-15 re-protonates (K_2), thus inhibiting proton transfer off the cluster. In the native protein, $pK_{ox} = 5.4$. Rate expressions are shown in the legend to Table 1.

serves as a proton *courier* in the manner of the 'swinging arm' mechanism proposed by Williams.[16]

While the *A.v.* FdI system provides a detailed model, the physiological relevance of the proton-coupling is not clear. The best established proton-coupling reaction of an iron-sulfur cluster is that of the so-called Rieske centre ($[2Fe\text{-}2S]^{2+/+}$) found in a subunit of the bc_1 complexes of mitochondria and bacteria, plant chloroplasts (b_6f) and several other enzymes. Proton coupling stems from the replacement of both cysteines by histidines at one of the Fe atoms, whereupon one or both of the imidazole side chains can deprotonate. This process has been studied extensively by Link and co-workers;[30] furthermore, during the preparation of this article a paper appeared describing experiments on the soluble Rieske fragment of the bc_1 complex from the thermophile *Thermus thermophilus*. Using film voltammetry, it has been possible to make measurements even up to pH 14, thereby gaining a surprisingly detailed picture of the proton-coupled redox thermodynamics.[31]

Changes in the oxidation state of an active site can also be linked to ligand exchange and associated conformational change. An example is the reductive activation of cytochrome cd_1 (a nitrite reductase) from *Paracoccus pantotrophus*, in which reduction of haem c causes one of its two axial histidine ligands to be replaced by methionine—the change being communicated to haem d (his/tyr axial ligation) causing the tyrosine to dissociate to give the five-coordinate catalytic state.[32] The chemistry at haem c is again described by a square scheme, in which his/his axial coordination is preferred for the oxidised form and his/met when reduced. This reaction has not been studied by voltammetry, but similar reactions occur at the small ET protein cytochrome c—either the native form under alkaline conditions, or in different mutants. These have been studied by voltammetric methods, although not in the adsorbed state (the reactions are slow enough to be resolved in solution voltammetry experiments with free protein).[33]

Another interesting system that has been studied recently is a mutant form of Azurin, in which one of the histidine residues (H117) coordinating the blue Cu atom has been changed to glycine.[34] The resulting 'cavity mutant' has a green colour in the Cu(II) state (an H_2O molecule is coordinated) but turns blue when imidazole is added, since free imidazole can be recruited in place of the absent side chain. However, in the reduced state, the Cu has a very low affinity for the imidazole (dissociation constant $K_{RED} > 14$ M) which is released rapidly. This chemistry, which is summarised in Scheme 3, is difficult to study by

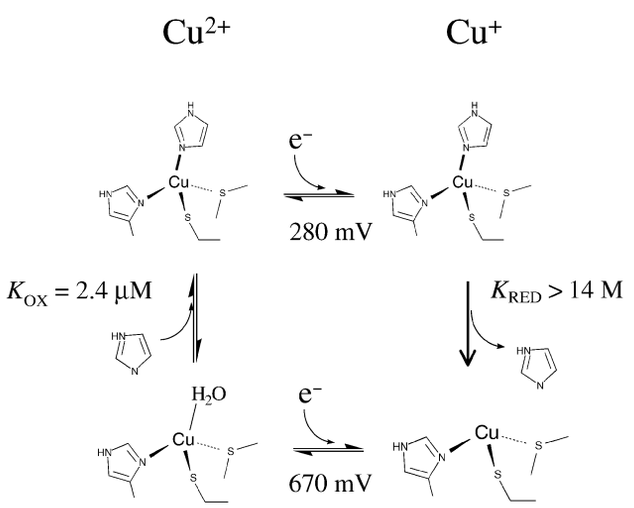

Scheme 3 Square scheme depicting the electrochemical reactions of H117G Azurin in the presence of exogenous imidazole. Imidazole binds tightly to the Cu(II) form of the active site, but the complex with the Cu(I) form is extremely weak and it dissociates rapidly after electron transfer.

conventional kinetic methods; however, it can be resolved by film voltammetry. The resulting trumpet plot is shown in Fig. 7, which includes the data obtained with a film of native azurin, for which ET is fast. At low scan rates, the redox transitions equilibrate mainly between imidazole-ligated Cu(II) and unligated Cu(I), and we note that the reduction potential is high, showing this to be a site that favours Cu(I). However, high scan rates (commencing the cycle from the oxidized form) trap the artificial 'blue' Cu system as a fast, reversible redox couple; notably with a reduction potential and electron-exchange kinetics that are similar to the native azurin. Evidently the protein framework is essential for retaining the imidazole sidechain in the Cu(I) state.

Measurement and interpretation of the potential-dependent catalytic activity of redox enzymes

Despite earlier skepticism, it is now established that many large redox enzymes display high rates of electron transfer and catalytic activity when adsorbed on an electrode, and there are obvious technological implications for electrocatalysis and

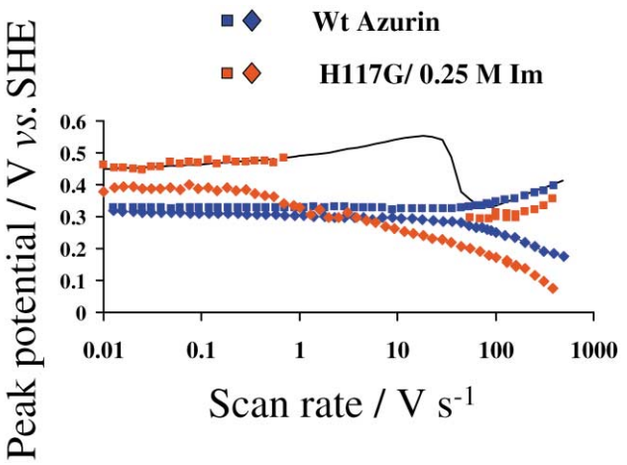

Fig. 7 'Trumpet Plots' for Azurin variants. Blue, wild type Azurin; Red, the H117 'cavity mutant' in the presence of 0.25 M imidazole. Temperature 0 °C, 0.15 M Na_2SO_4, pH 6.0. All cycles commenced from oxidative limit. Squares are oxidation peak positions, diamonds are reduction peak positions. The reduction potential of the H117G/ imidazole complex depends on the concentration of neutral imidazole. Adapted from *J. Am. Chem. Soc.*, 2000, **122**, 12186–12194 with permission. Copyright 2000 Am. Chem. Soc.

sensory devices. The most active system so far established is the hydrogenase from *Allochromatium vinosum*, which contains a novel binuclear NiFe centre as the buried active site, and three Fe-S clusters which provide a relay system to the protein surface.[35] The medial ([3Fe-4S]) cluster in this series has a much higher reduction potential than the proximal or distal [4Fe-4S] clusters, and this has raised interest with regard to whether the 'uphill' ET step is detrimental to catalysis.[36] Hydrogenase can be adsorbed onto a PGE electrode, at which it catalyses the oxidation of hydrogen or reduction of water.[35] As shown in Fig. 8, oxidation of H_2 is diffusion-controlled (the turnover

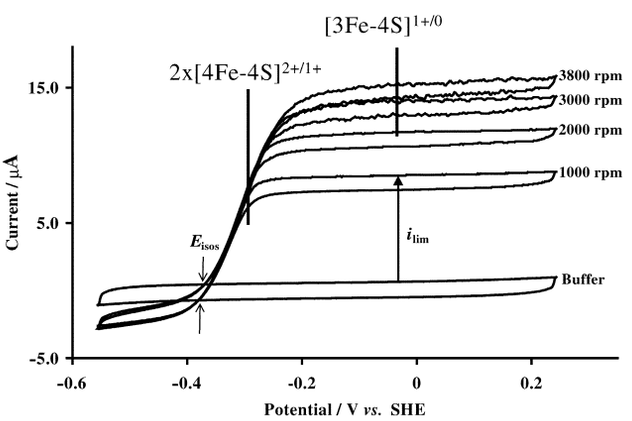

Fig. 8 Cyclic voltammograms of *Allochromatium vinosum* NiFe hydrogenase adsorbed on a rotating disc PGE electrode under an atmosphere of 10% H_2 in N_2. Temperature 30 °C, pH 6.5, scan rate 0.1 V s^{-1}. Adapted from *Biochemistry*, 1999, **38**, 8992–8999. Copyright 1999 Am. Chem. Soc.

number easily exceeds 1500 s^{-1} at 35 °C) and this high activity makes it difficult to determine features of the mechanism. One aspect worth noting is that the activity is high even at potentials where the [3Fe-4S] cluster should remain close to 100% reduced during the steady state.

The clearest picture so far of an active redox enzyme on an electrode surface stems from studies we have made with fumarate reductase (FRD), which catalyses the reduction of fumarate to succinate—a terminal reaction in the respiratory chain of *Escherichia coli* growing under anaerobic conditions.[37] The crystal structure of this membrane-bound enzyme (MW > 100 kDa) was solved recently.[38] It is closely related to succinate

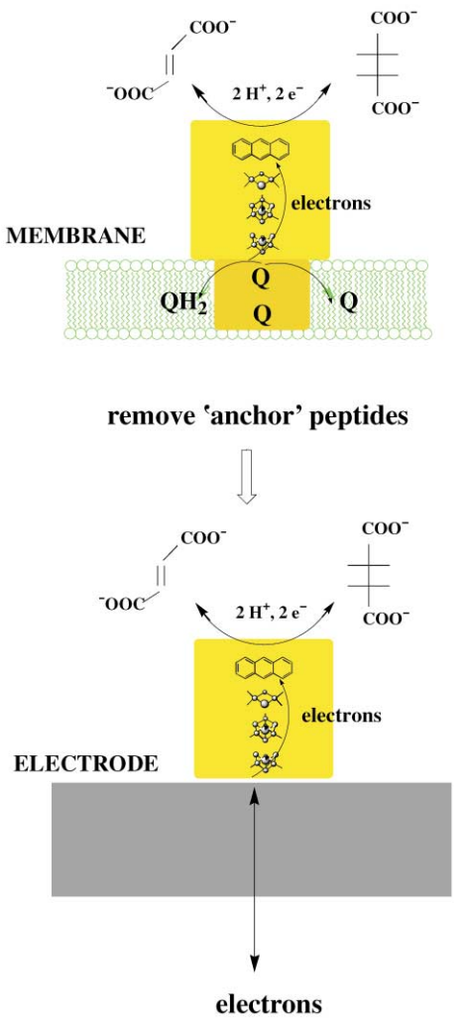

Fig. 9 Cartoon showing succinate–fumarate quinone oxidoreductases: first as membrane-bound enzymes, then as soluble forms (SDH or FRD) free of membrane 'anchor' peptides and adsorbed on an electrode which replaces the quinone/quinol pool by a variable potential. The soluble, membrane-extrinsic sub-complex contains the FAD and Fe-S centres 1, 2 and 3. The membrane-intrinsic 'anchor' peptides contain two bound quinones.

dehydrogenase (SDH) which, as Complex II of mitochondria, links the citric acid cycle to the membrane-bound respiratory chain.

The cartoon in Fig. 9 shows that FRD and SDH are associated with energy-transducing membranes, as membrane-extrinsic domains attached to hydrophobic 'anchor' peptides. However, either by chemical or genetic means, both enzymes can be isolated in soluble forms (free of the membrane 'anchor' peptides) that retain catalytic activity with water-soluble redox partners.[37] The soluble enzymes comprise two tightly-bound subunits, one containing the catalytic site and featuring a covalently-bound flavin (FAD), and the other containing three Fe-S clusters (centre 1, [2Fe-2S]; centre 2, [4Fe-4S]; and centre 3, [3Fe-4S]). These Fe-S clusters relay electrons between the FAD and the quinol/quinone 'pool' that is confined to the membrane. These soluble enzymes can be adsorbed at a PGE electrode (Fig. 9, bottom) and it is interesting and important to note that the electrode effectively replaces the membrane-bound quinone pool by a variable potential source.[39–45]

As shown in Fig. 10 (top), FRD adsorbed at PGE gives rise to a complex voltammogram that can be deconvoluted into four signals, each of which may be assigned to a particular redox centre on the basis of earlier potentiometric studies monitored by spectroscopy.[39,40] The coverage is approximately as expected for a monolayer, and we note the ability of protein film voltammetry to detect redox centres in large enzymes. The most

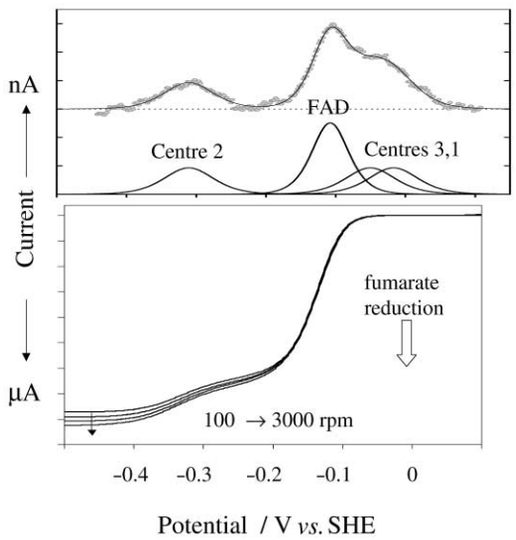

Fig. 10 Voltammetry of a film of *E. coli* fumarate reductase adsorbed on a PGE electrode at pH 9, 25 °C. Top: Baseline-corrected voltammogram (only the oxidative sweep is shown) and deconvolution showing the individual redox centres. The FAD is particularly prominent. Bottom: Voltammetry after addition of fumarate (0.2 mM) and rotation of the electrode. Note the boost in current observed close to the potential of the [4Fe-4S] cluster.

prominent feature is the FAD which is sharp (since $n > 1$) and integrates to twice the intensity of the signals from the three Fe-S clusters. The FAD potential is much more pH sensitive than the Fe-S clusters: the voltammogram in Fig. 10 (top) was measured at pH 9, and two of the Fe-S clusters (centres 1 and 3, *i.e.* [2Fe-2S] and [3Fe-4S]) appear as a high-potential shoulder. The third Fe-S cluster (centre 2, [4Fe-4S]) has a more negative reduction potential (and similar to hydrogenase) this raises again the question of what difference this makes to intramolecular electron transport rates and catalytic efficiency.[36]

Addition of fumarate causes the signal to convert to a catalytic wave (Fig. 10, bottom) and by analysing the concentration and rotation rate dependencies, the kinetic constants can be verified to be similar to those obtained from conventional methods. At pH 7, the enzyme is very active and catalytic currents depend greatly on electrode rotation rate. By contrast, at pH 9, the enzyme is much less active for fumarate reduction, and the catalytic current is almost insensitive to rotation rate. Catalytic electron transport under these conditions is therefore controlled by properties of the enzyme, not by mass transport of substrate. The voltammogram is not the simple sigmoid that was anticipated from Fig. 2C, and we note the appearance of a second wave at a potential coinciding with reduction of the low-potential [4Fe-4S] cluster. The origin of this activity boost remains to be established: one possibility is that some enzyme molecules are oriented so that the best connection is made with the [4Fe-4S] cluster rather than with [3Fe-4S] which is normally proximal to the membrane.[38] However, it does raise the question of whether something more fundamental is being revealed; for example is there an enhanced ability of the reduced cluster to support a super-exchange ET process or does the redox state of the [4Fe-4S] cluster influence the catalytic properties of the active site?

Succinate dehydrogenase isolated from beef heart mitochondria is inactivated easily in air: however under anaerobic conditions it can be adsorbed at a PGE electrode at which it shows activity.[41–45] So far we have been unsuccessful in achieving more than a low coverage film, which, unlike FRD, does not reveal signals due to the different redox centres. Succinate dehydrogenase catalyses the oxidation of succinate, as expected: however an unusual property is revealed in the direction of fumarate reduction, in that the voltammograms (which are insensitive to electrode rotation rate) show a peak-like waveform. The voltammetry is unstable, and although this might be expected to be a disadvantage, it actually provides a convenient way to analyse the voltammetry if both succinate and fumarate are present in the cell solution. Successive cycles (with oxidation and reduction currents decreasing simultaneously) trace out an isosbestic point, the potential of which is equal to the formal reduction potential of the fumarate/succinate system.[43] Subtracting a late voltammogram from an early one produces the Faradaic current/potential profile shown in Fig. 11, in which the

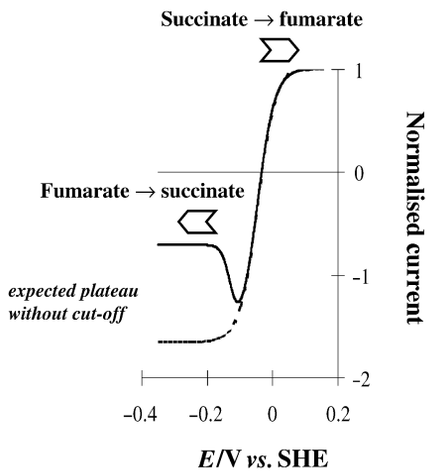

Fig. 11 Voltammetry of succinate dehydrogenase adsorbed as a dilute film on a PGE electrode, and catalysing interconversion of a mixture of fumarate and succinate. The voltammogram was obtained by subtracting a 'late' from an 'early' voltammogram, as the voltammetry decays with time. The broken line indicates how the fumarate reduction current would appear in the absence of the cut-off.

isosbestic potential provides a good reference point for analysing the energetics of catalysis, including H/D isotope effects.[44]

The rate of fumarate reduction increases as the potential is lowered, but reaches a maximum value (the 'cut-off') beyond which it decreases quite sharply despite the increase in electrochemical driving force. In terms of electron flow, the effect resembles that of an electronic device known as a tunnel diode, which displays negative resistance in a certain region of potential bias.[41] That the potential dependence of the cut-off stems from an intrinsic property of the enzyme rather than from a change in the state of the electrode or electrical double layer stems from several lines of evidence.[42,45] Firstly, at a gold electrode, the beef heart enzyme gives a weak and unstable catalytic response, but nonetheless with the same shape and potential values as observed at a PGE electrode.[42] Secondly, steady-state kinetic studies on SDH using conventional solution methods reveal that the enzyme-catalysed oxidation of benzyl viologen by fumarate *accelerates* rather than slows down during the course of the reaction.[42] The interpretation is that as benzyl viologen is consumed, the potential rises and the enzyme becomes more active, as predicted by the voltammetry. Thirdly, studies with *E. coli* SDH, which has only 50% similarity with the beef heart enzyme (the homology is concentrated in the region where the FAD binds) give a very similar result; although, in this case the cut-off is almost total, *i.e.* the current drops to nearly zero at negative potentials.[45] Finally, the same behaviour is noted for SDH from different organisms, but not for those enzymes formally classified as fumarate reductases on the basis of their assumed biological function.[42] An explanation for the potential dependence of activity is that the active site exists in two conformations depending on the oxidation state of the FAD. The more active conformation is associated with the oxidized form, which persists at higher potentials, while application of a more negative potential favours the less active reduced form and the catalytic current for fumarate reduction decreases despite the more favourable driving force.

The conclusion from the voltammetry studies is that SDH is a very good catalyst of fumarate reduction (our studies show that at pH 7, it is actually biased to catalyse in this direction), but the activity is optimised only within a narrow region of potential. The fumarate ↔ succinate interconversion may be an important point for metabolic regulation: that is, SDH could serve to regulate or synchronise mitochondrial electron transport with respect to the citric acid cycle reactions, in feedback response to the potential of the environment in the mitochondria (*e.g.* the quinone/quinol ratio).

Related behaviour has been noted in the catalytic electrochemistry of other enzymes. An interesting case is DMSO reductase (DMSO, dimethylsulfoxide = $(CH_3)_2SO$) from *E. coli*, which contains a Mo bis(pterin) centre and four [4Fe-4S] clusters.[46] Like fumarate reductase, this large, membrane-bound enzyme catalyses a terminal reaction of anaerobic respiration, in this case the reduction of DMSO to DMS ($(CH_3)_2S$). The crystal structure is not yet known, but it is certain that the Mo centre is the site at which DMSO is reduced (most likely by an oxo-transfer mechanism, involving cycles between Mo(IV) and Mo(VI)), and it is assumed that the electrons are supplied by quinol molecules in the cytoplasmic membrane and transferred sequentially to Mo (VI ⟶ V ⟶ IV) using the four Fe-S clusters. The enzyme can be adsorbed onto a PGE electrode where it catalyses the conversion of DMSO to DMS, and like SDH, the steady-state voltammetry shows a peak-type catalytic reduction wave.[46] Unlike SDH, DMSO reductase does not function in the reverse direction; but studies carried out using the oxyphilic substrate trimethylphosphine (PMe_3) reveal an oxidation current, the waveform of which is also peak-like, so that activity drops to zero above a certain potential. The activity profile is summarised in Fig. 12, from which the two electrocatalytic

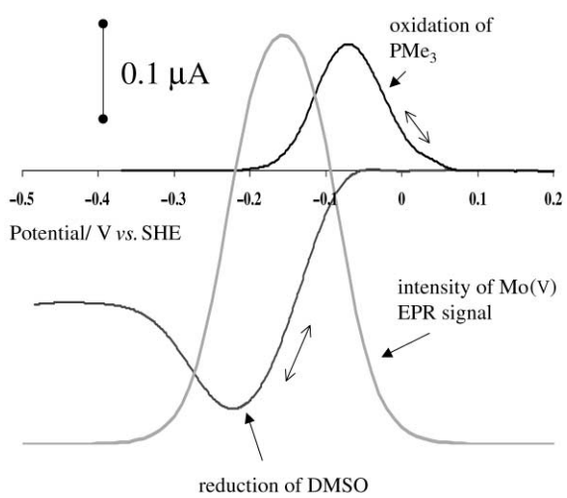

Fig. 12 Voltammograms showing catalysis of DMSO reduction or PMe_3 oxidation by molecules of DMSO reductase adsorbed on a PGE electrode (conditions pH 9, 25 °C) and comparison with the appearance of a Mo(V) EPR signal during a potentiometric titration. Reproduced with permission from *Biochemistry*, 2001, **40**, 3117–3126. Copyright 2001 Am. Chem. Soc.

peaks, for oxidation and reduction, suggest that the enzyme's activity is restricted to a narrow 'window' of electrochemical potential.

The origin of this effect poses more problems than for SDH since it is difficult to set up alternative, non-electrochemical experiments to test how activity varies with driving force. No activity could be observed using other electrodes, apart from basal plane graphite, at which similar voltammetry is observed. However, an interesting clue to the origin of this effect was provided by comparing the 'window of potential' with the potential dependence for the observation of the EPR signal due to Mo(V). Fig. 12 shows also that the window of activity defined by the oxidation of PMe_3 or DMSO fits very nicely either side of the titration curve for Mo(V).[46] The explanation that we have proposed, based on observations and measurements at different pH values and DMSO concentrations, is that the crucial events in the catalytic cycle are facilitated at the stage where the active site is in the intermediate Mo(V) oxidation state. This hypothesis, depicted in Scheme 4, is interesting

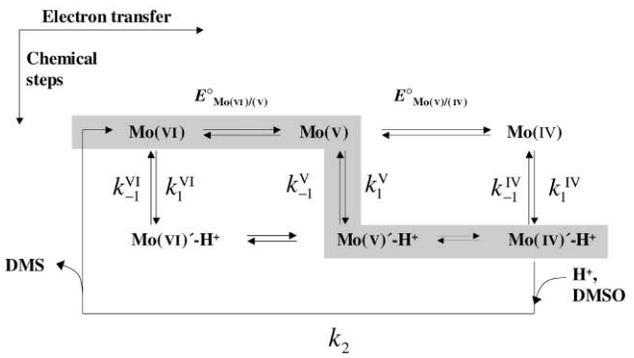

Scheme 4 Catalytic pathway proposed for reduction of DMSO by DMSO reductase, accounting for the faster rate observed if the active site Mo centre is constrained by the electrode potential to remain predominantly in the (V) oxidation state. The proposal requires that essential parts of the catalytic cycle (k^{V}_{1} and k^{V}_{-1}) occur more rapidly in this form. Reproduced with permission from *Biochemistry*, 2001, **40**, 3117–3126. Copyright 2001 Am. Chem. Soc.

because it supports a specific function for the EPR-detectable Mo(V) state in substrate binding/transformation, rather than being just an intermediate in the completion of the catalytic cycle by one-electron transfers from the secondary redox partner. As this article was being prepared, there appeared a report on a related Mo enzyme, the nitrate reductase from *Paracoccus pantotrophus*.[47] In this case, like DMSO reductase, there is striking evidence that catalytic activity is optimised at a certain potential and once again this may reflect an important role played by the Mo(V) state.

Conclusions

This article has described a few examples in which voltammetric studies of proteins that are tightly bound to an electrode surface reveal interesting and intricate chemistry that is not detected easily or at all by other methods. I have restricted the discussion to studies in which my group and I have been involved, and some aspects have been omitted such as applications of protein film voltammetry to unravel Fe-S cluster interconversions and oxidative damage mechanisms.[48] It is important to acknowledge the advances being made by other groups, such as Bowden (proteins adsorbed on self-assembled alkanethiol monolayers),[9] Rusling (enzymes embedded in surfactant films),[4] Farmer (myoglobin-based models for nitrogen cycle enzymes),[49] Niki (electroreflectance),[3] Hildebrandt (surface-enhanced resonance Raman spectroscopy),[2,12] Hirst (the Rieske Fe-S centre),[31] Butt (nitrate reductase)[47] and Dutton (cytochrome c oxidase).[50] Protein film voltammetry is proving to be an excellent investigative technique, and we should be confident of its future. The science of proteins at electrodes is destined to produce some exciting future developments across a wide range of interests, spanning the fields of electrochemistry, catalysis, biosensors, surface and interface science, nanostructures, bioenergetics and enzymology.

Acknowledgements

I would like to thank numerous colleagues for their enthusiastic input throughout the past years. In particular, Julea Butt, Artur Sucheta, Barbara Burgess, Brian Ackrell, Judy Hirst, Jill Duff, Dirk Heering, Harsh Pershad, Raul Camba, Kerensa Heffron,

Christophe Léger, Lars Jeuken, James McEvoy, Sean Elliott, Richard Rothery, Joel Weiner, Siem Albracht and Gerard Canters have each contributed to the studies that I have summarised above. I am grateful also to Professor Allen Hill who first interested me in the field of bioelectrochemistry and Alan Bond who convinced me that protein diffusion was a major obstacle. Research has been supported over the past ten years by the UK EPSRC and BBSRC, The Wellcome Trust, The Royal Society, Exxon Education Foundation, The Petroleum Research Fund, National Science Foundation, NATO, and the Human Frontier Science Program.

References

1 F. A. Armstrong, H. A. Heering and J. Hirst, *Chem. Soc. Rev.*, 1997, **26**, 169.
2 S. Lecompte, H. Wackerbarth, T. Soulimane, G. Buse and P. Hildebrandt, *J. Am. Chem. Soc.*, 1998, **120**, 7381.
3 Z. Q. Feng, S. Imabayashi, T. Kakiuchi and K. Niki, *J. Electroanal. Chem. Interfacial Electrochem.*, 1995, **394**, 149.
4 A.-E. Nassar, Z. Zhang, N. Fu and J. F. Rusling, *J. Phys. Chem. B.*, 1997, **101**, 2224.
5 E. Laviron, in *Electroanalytical Chemistry*, ed. A. J. Bard, 1982, Marcel Dekker, New York, vol. 12, p. 53.
6 A. M. Bond and K. B. Oldham, *J. Phys. Chem.*, 1983, **87**, 2492.
7 H. A. Heering, J. Hirst and F. A. Armstrong, *J. Phys. Chem. B.*, 1998, **102**, 6889.
8 F. A. Armstrong, P. A. Cox, H. A. O. Hill, V. J. Lowe and B. N. Oliver, *J. Electroanal. Chem. Interfacial Electrochem.*, 1987, **217**, 331.
9 A. El Kasmi, J. M. Wallace, E. F. Bowden, S. M. Binet and R. J. Linderman, *J. Am. Chem. Soc.*, 1998, **120**, 225.
10 Q. Feng, S. Imabayashi, T. Kakiuchi and K. Niki, *J. Chem. Soc., Faraday Trans.*, 1997, **93**, 1367.
11 V. L. Davidson, *Acc. Chem. Res.*, 2000, **33**, 87.
12 D. H. Murgida and P. Hildebrandt, *J. Am. Chem. Soc.*, 2001, **123**, 4062.
13 Q. J. Chi, J. D. Zhang, J. E. T. Andersen and J. Ulstrup, *J. Phys. Chem. B.*, 2001, **105**, 4669.
14 H. D. Sikes, J. F. Smalley, S. P. Dudek, A. R. Cook, M. D. Newton, C. E. D. Chidsey and S. W. Feldberg, *Science*, 2001, **291**, 1519.
15 L. I. Krishtalik, *Biochim. Biophys. Acta*, 2000, **1458**, 6.
16 R. J. P. Williams, *J. Theor. Biol.*, 1961, **1**, 1.
17 J. R. Fetter, J. Qian, J. Shapleigh, J. W. Thomas, A. Garcia-Horsman, E. Schmidt, J. Hosler, G. T. Babcock, R. B. Gennis and S. Ferguson-Miller, *Proc. Natl. Acad. Sci. USA*, 1995, **92**, 1604.
18 B. Shen, L. L. Martin, J. N. Butt, F. A. Armstrong, C. D. Stout, G. M. Jensen, P. J. Stephens, G. N. La Mar, C. M. Gorst and B. K. Burgess, *J. Biol. Chem.*, 1993, **268**, 25928.
19 J. Hirst, J. L. C. Duff, G. N. L. Jameson, M. A. Kemper, B. K. Burgess and F. A. Armstrong, *J. Am. Chem. Soc.*, 1998, **120**, 7085.
20 K. Chen, J. Hirst, R. Camba, C. A. Bonagura, C. D. Stout and F. A. Armstrong, *Nature*, 2000, **405**, 814.
21 F. A. Armstrong, S. J. George, A. J. Thomson and M. G. Yates, *FEBS Lett.*, 1988, **234**, 107.
22 S. J. George, A. J. M. Richards, A. J. Thomson and M. G. Yates, *Biochem. J.*, 1984, **224**, 247.
23 P. J. Stephens, G. M. Jensen, F. J. Devlin, T. V. Morgan, C. D. Stout, A. E. Martin and B. K. Burgess, *Biochemistry*, 1991, **30**, 3200.
24 D. Bentrop, I. Bertini, M. Borsari, G. Cosenza, C. Luchinat and Y. Niikura, *Angew. Chem., Int. Ed.*, 2000, **39**, 3620.
25 C. D. Stout, *J. Biol. Chem.*, 1993, **268**, 25920.
26 C. D. Stout, E. A. Stura and D. E. McRee, *J. Mol. Biol.*, 1998, **278**, 629.
27 C. G. Schipke, D. B. Goodin, D. E. McRee and C. D. Stout, *Biochemistry*, 1999, **38**, 8228.
28 J. Hirst and F. A. Armstrong, *Anal. Chem.*, 1998, **70**, 5062.
29 M. Lübben, A. Prutsch, B. Mamat and K. Gerwert, *Biochemistry*, 1999, **38**, 2048.
30 T. A. Link, *Adv. Inorg. Chem.*, 1999, **47**, 83.
31 Y. Zu, J. A. Fee and J. Hirst, *J. Am. Chem. Soc.*, 2001, **123**, 9906.
32 A. Koppenhöfer, K. L. Turner, J. W. A. Allen, S. K. Chapman and S. J. Ferguson, *Biochemistry*, 2000, **39**, 4243.
33 B. A. Feinberg, X. Liu, M. D. Ryan, A. Schejter, C. Zhang and E. Margoliash, *Biochemistry*, 1998, **37**, 13091.
34 L. J. C. Jeuken, P. van Vliet, M. Ph. Verbeet, R. Camba, J. P. McEvoy, F. A. Armstrong and G. W. Canters, *J. Am. Chem. Soc.*, 2000, **122**, 12186.
35 H. R. Pershad, J. L. C. Duff, H. A. Heering, E. C. Duin, S. P. J. Albracht and F. A. Armstrong, *Biochemistry*, 1999, **38**, 8992.
36 C. C. Page, C. C. Moser, X. X. Chen and P. L. Dutton, *Nature*, 1999, **402**, 47.
37 B. A. C. Ackrell, M. K. Johnson, R. P. Gunsalus and G. Cecchini, in *Chemistry and Biochemistry of Flavoenzymes*, ed. F. Müller, 1992, CRC Press, Boca Raton, Florida, vol. 3, p. 229.
38 T. M. Iverson, C. Luna-Chavez, G. Cecchini and D. C. Rees, *Science*, 1999, **284**, 1961.
39 A. Sucheta, R. Cammack, J. H. Weiner and F. A. Armstrong, *Biochemistry*, 1993, **32**, 5455.
40 H. A. Heering, J. H. Weiner and F. A. Armstrong, *J. Am. Chem. Soc.*, 1997, **120**, 11628.
41 A. Sucheta, B. A. Ackrell, B. Cochran and F. A. Armstrong, *Nature*, 1992, **356**, 361.
42 B. A. C. Ackrell, F. A. Armstrong, B. Cochran, A. Sucheta and T. Yu, *FEBS Lett.*, 1993, **326**, 92.
43 J. Hirst, A. Sucheta, B. A. C. Ackrell and F. A. Armstrong, *J. Am. Chem. Soc.*, 1996, **118**, 5031.
44 J. Hirst, B. A. C. Ackrell and F. A. Armstrong, *J. Am. Chem. Soc.*, 1997, **119**, 7434.
45 H. R. Pershad, J. Hirst, B. Cochran, B. A. C. Ackrell and F. A. Armstrong, *Biochim. Biophys. Acta*, 1999, **1412**, 262.
46 K. Heffron, C. Léger, R. A. Rothery, J. H. Weiner and F. A. Armstrong, *Biochemistry*, 2001, **40**, 3117.
47 L. J. Anderson, D. J. Richardson and J. N. Butt, *Biochemistry*, 2001, **40**, 11294.
48 R. Camba and F. A. Armstrong, *Biochemistry*, 2000, **39**, 10587.
49 M. Bayachou, R. Lin, W. Cho and P. J. Farmer, *J. Am. Chem. Soc.*, 1998, **120**, 9888.
50 A. S. Haas, D. L. Pilloud, K. S. Reddy, G. T. Babcock, C. C. Moser, K. K. Blasie and P. L. Dutton, *J. Phys. Chem. B*, 2001, **105**, 11351.